



OPEN

Long-term fungal inoculation of *Ficus sycomorus* and *Tectona grandis* woods with *Aspergillus flavus* and *Penicillium chrysogenum*

Maisa M. A. Mansour^{1✉}, Wafaa A. Mohamed¹, Ahmed A. A. El-Settawy², Martin Böhm³, Mohamed Z. M. Salem^{2✉} & Marwa G. S. Farahat²

In the current study, two molds, *Aspergillus flavus* (ACC# LC325160) and *Penicillium chrysogenum* (ACC# LC325162) were inoculated into two types of wood to be examined using scanning electron microscopy-energy dispersive X-ray (SEM–EDX) and computerized tomography (CT) scanning. *Ficus sycomorus*, a non-durable wood, and *Tectona grandis*, a durable wood, were the two wood blocks chosen, and they were inoculated with the two molds and incubated for 36 months at an ambient temperature of 27 ± 2 °C and $70 \pm 5\%$ relative humidity (RH). The surface and a 5-mm depth of inoculated wood blocks were histologically evaluated using SEM and CT images. The results showed that *A. flavus* and *P. chrysogenum* grew enormously on and inside of *F. sycomorus* wood blocks, but *T. grandis* wood displayed resistance to mold growth. The atomic percentages of C declined from 61.69% (control) to 59.33% in *F. sycomorus* wood samples inoculated with *A. flavus* while O increased from 37.81 to 39.59%. *P. chrysogenum* caused the C and O atomic percentages in *F. sycomorus* wood to drop to 58.43%, and 26.34%, respectively. C with atomic percentages in Teak wood's C content fell from 70.85 to 54.16%, and 40.89%, after being inoculated with *A. flavus* and *P. chrysogenum*. The O atomic percentage rose from 28.78 to 45.19% and 52.43%, when inoculated with *A. flavus* and *P. chrysogenum*, respectively. Depending on how durable each wood was, The examined fungi were able to attack the two distinct types of wood in various deterioration patterns. *T. grandis* wood overtaken by the two molds under study appears to be a useful material for a variety of uses.

Numerous wood species, including *Ficus sycomorus*, *Cedrus libani*, *Quercus cerris*, *Zizyphus spina Christi*, and *Tamarix* sp. have been discovered in ancient Egyptian tombs¹. The studied samples revealed varying preservation conditions in terms of carbohydrate and/or lignin loss despite their long-term burial in dry archaeological sites. High concentrations of soluble chemicals made it difficult to interpret the findings. These water-soluble substances contained depolymerized lignin or carbohydrates². It is commonly known that wood, an organic natural material, is vulnerable to attack by fungi when the right conditions exist, such as when moisture content raises to 20% and temperature falls between 25 and 40 °C^{3–9}.

When fungi invade wood, they consume its elemental composition and carbohydrates. Brown and white rot attack by depolymerizing the layers of the cell wall, whereas soft-rot fungi create cavities in the secondary wall^{3,10}. Fungal growth and reproduction utilize starch and simple sugars contained in the structure, particularly in ray and axial parenchyma cells lumen, which results in structural changes of the wooden objects¹⁰. Fungi create extracellular enzymes, such as cellulase, xylanase, and α -l-arabinofuranosidase, as they multiply and colonize wood in a dynamic and competitive process^{11–16}. They can also grow in wood's longitudinal, radial, and tangential orientations^{17–19}. The hyphae can pass between the wood rings, into the cell wall, between fibers, and through pits^{18,20–22}.

The *Penicillium*, *Paecilomyces*, and *Aspergillus* genera of molds, can deteriorate wood and wood products⁷. Cellulase and other extracellular enzymes produced by *Penicillium* species²³, break down pectin and xylan²⁴.

¹Department of Conservation and Restoration, Faculty of Archaeology, Cairo University, Giza 12613, Egypt. ²Forestry and Wood Technology Department, Faculty of Agriculture (El-Shatby), Alexandria University, Alexandria 21545, Egypt. ³Department of Materials Engineering and Chemistry, Faculty of Civil Engineering, Czech Technical University in Prague, Thákurova 7, 166 29 Prague 6, Czech Republic. ✉email: maisamansour@cu.edu.eg, mohamed-salem@alexu.edu.eg

Paecilomyces variotii, the soft-rot fungus, produces amylase enzyme²⁴. The xylanases enzyme^{24,25} and hydrolytic enzymes that can break down hemicelluloses and cellulose²⁶, are produced by *Aspergillus* species. Although some molds, like *Trichoderma viride*, do not decompose wood, they do enzymatically consume the nutrients found in the parenchyma cells²⁷.

After 4 years of colonization in *Acacia saligna* wood, *Aspergillus niger*, *A. flavus*, *Alternaria tenuissima*, *Fusarium culmorum*, and *T. harzianum* revealed checks and breaks inside the secondary cell wall regions, which were caused by the action of acids on polysaccharides²⁸. *T. viride* and *A. alternata*, a surface mold fungi, have the ability to alter the ultrastructure of wood similarly to soft-rot fungi⁸.

Cellulase enzymes are secreted by the lignocellulolytic fungi of the genera *Aspergillus* and *Penicillium*, which hydrolyze cellulose to produce glucose, a monosaccharide molecule⁴. *Penicillium chrysogenum* is another fungus that rots wood; its hyphae are closely attached to the structure of the wood, and erosion troughs developed in the wood's deteriorating cell walls in soil^{5,8}. Amorphous cellulose and xylan (hemicellulose) breakdown in wood has been retained in dry conditions and over an extended length of time²⁹. Dry ancient wood degrades more complexly than waterlogged wood².

Among the traditional examination methods, Computed tomography (CT), one of the more common examination techniques, has the potential to be a tool for measuring the depth of fungal penetration in wood. CT generates cross-sectional (tomographic) images (virtual "slices") from various angles of specific areas, allowing a nondestructive closer look at fungal growth within wood structures^{30–32}.

This research looked at how *Aspergillus flavus* and *Penicillium chrysogenum* affected *Ficus sycomorus* and *Tectona grandis* after being inoculated over a 36-month period.

Materials and methods

Wood samples. This study has complied with relevant institutional, national, and international guidelines and legislation. This study does not contain any studies with human participants or animals performed by any of the authors. Sapwood samples of *Ficus sycomorus*, a 25-year-old native tree species, and *Tectona grandis*, an imported wood³³, were both used as sources of wood. In a wood workshop in Alexandria, Egypt, ten woodblock samples from *F. sycomorus* and *T. grandis* were prepared with dimensions of 0.5 × 1 × 2 cm, autoclaved at 121 °C and then dried in an oven at 103 ± 2 °C for 24 h^{34,35}.

Tested fungi. For the wood inoculation, two soft-rot fungi *Aspergillus flavus* and *Penicillium chrysogenum*, were used. These fungi were previously molecularly identified and deposited in the GenBank under the accession numbers LC325160, and LC325162, respectively.

Inoculation of wood samples with the tested fungi. Each piece of wood sample was individually inoculated in Petri plates with media of potato dextrose agar (PDA) and fungus discs from *A. flavus* (ACC# LC325160), and *P. chrysogenum* (ACC# LC325162) measuring 5 mm in diameter^{9,36}. Following this, fungi were cultured on wood blocks under experimental conditions (27 ± 2 °C and 70 ± 5% relative humidity (RH)), where the incubation lasted until the complete colonization of the fungus on the Petri dishes and wood block. After this time, Petri plates were covered a plastic wrap made of cling film and stored in a growth chamber for 36 months at the ambient conditions (27 ± 2 °C and 70 ± 5% RH)²⁸. The inoculated woodblocks were then removed for additional examination.

SEM–EDX examination of the inoculated wood samples. Using an environmental scanning electron microscope (ESEM) (Quanta FEG250; FEI Co., Hillsboro, OR, USA), the inoculated wood samples of *F. sycomorus* and *T. grandis* were analyzed for the fungal infestation (*A. flavus* and *P. chrysogenum*) on the surface and at 5-mm depth of the infected wood block. Energy dispersive spectroscopy (ESEM–EDS (Quanta FEG250; FEI Co., Hillsboro, OR, USA, with tungsten electron source, at 20 kV) was used to examine the variations in surface elemental compositions.

CT scanning examination. The hyphal fungal infestation within the tested wood samples was examined by X-ray computed tomography (CT) scanning using a Toshiba Aquilion 16 CT Scanner, Tokyo, Japan. Using 3-D imaging, which is an image quality with surface shaded-renderings and volume-rendered 3-D images, datasets were displayed and images and videos were recorded. Distance measurements were made as the 3-D surface was zoomed in and out. The Aquilion 16 features 896 channels in 40 rows of solid-state detectors with a variety of slice thicknesses was used to test high image quality. In the x, y, and z directions, the system had a low-contrast resolution of 2 mm at 0.3% and a high-contrast resolution of 0.35 mm. The following values were used: voltage 120 kV, current 150 mA, timing 15.819 s, and thickness 0.5 × 16 mm²³⁷. The CT number, which is expressed by brightness data in an image, is based on linear X-ray absorption coefficients³⁸.

Results and discussion

SEM and CT scanning examination results of fungal inoculated *Ficus sycomorus* wood. On *Ficus sycomorus* wood, *Aspergillus flavus* growth was clearly visible in all samples (Fig. 1). A visual augmentation in conidia quantity was observed at different areas with several aerial fungal mycelium and conidia covered the surface of *F. sycomorus* in various locations, causing a visible increase in conidia abundance (Fig. 1a and b). Additionally, conidiospores and mycelium quantity increased as a result of aberrant spore development along the hyphae in the basal mycelium (Fig. 1c and d).

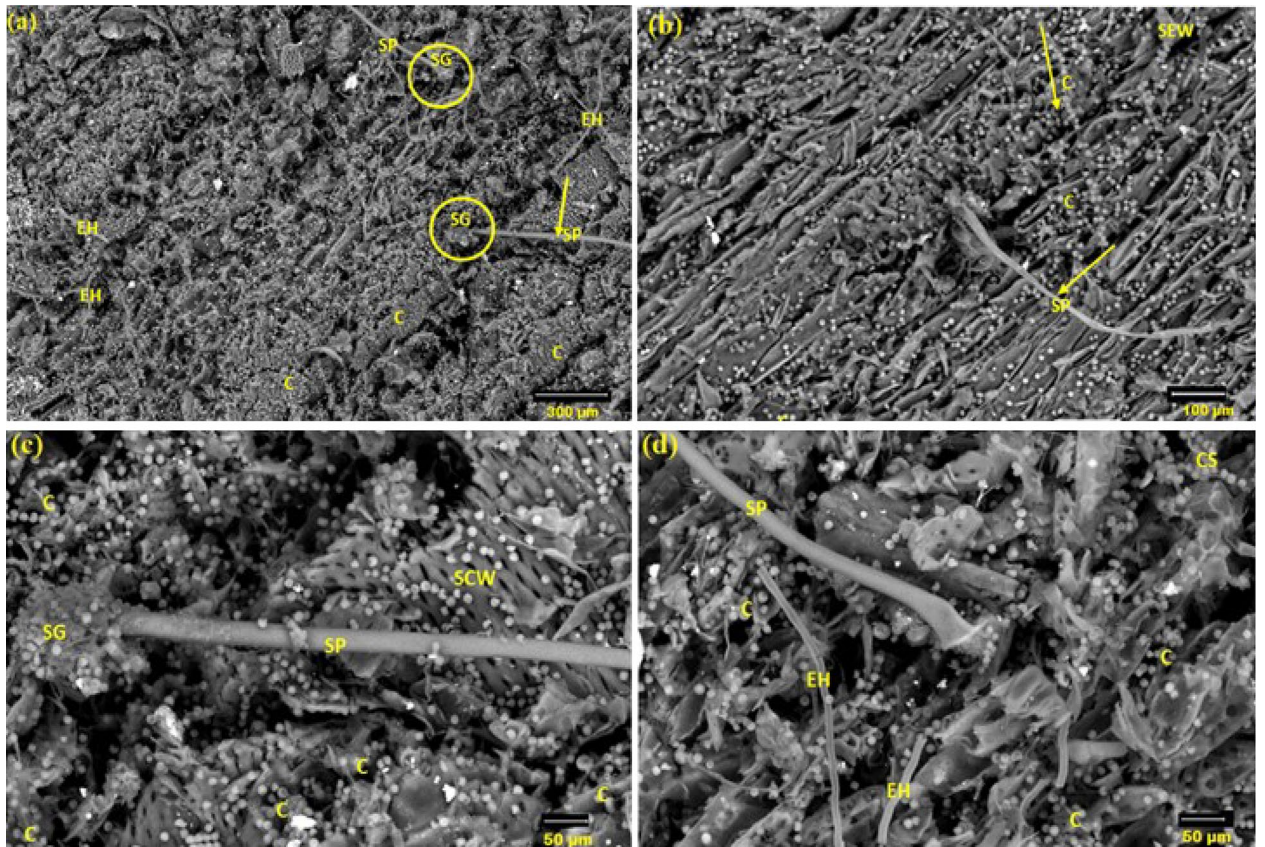


Figure 1. SEM images of wood samples from *F. sycomoros* that have been inhabited by the rapid growth of *A. flavus*. A number of aerial fungal mycelium are displayed in (a), conidia are distributed, sporangiophore and conidia are displayed, and the fungus' exterior hyphae are displayed in (b–d). SG sporangium, CS conidiospores, EH external hyphae, SP sporangiophore, SCW secondary cell wall, C conidia.

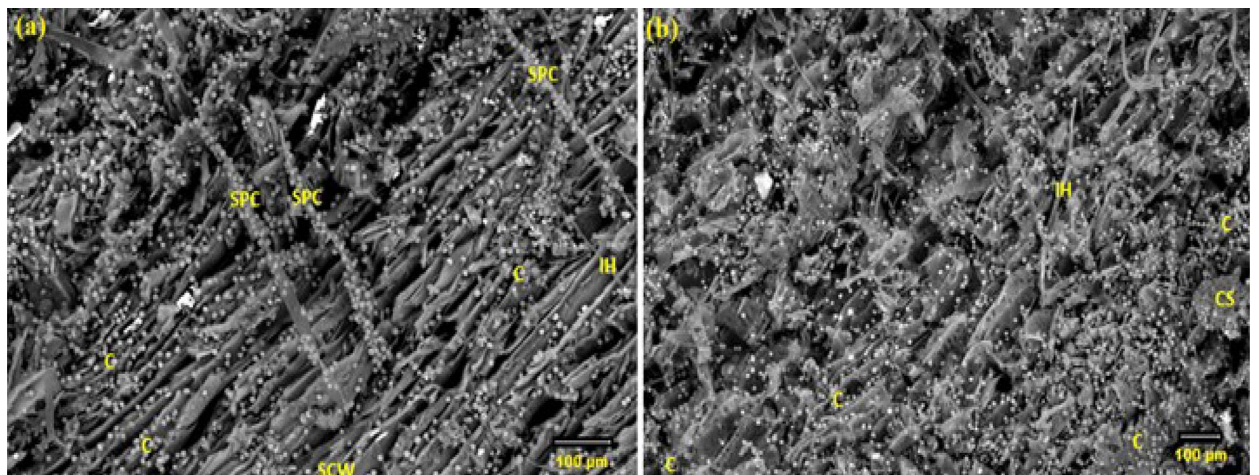


Figure 2. An SEM image of the infected *F. sycomoros* wood (5-mm depth) with *A. flavus* reveals the spore, the growth morphology of the hyphae within the wood fibers, and the penetration of hyphae inside the wood and within cells due to *A. flavus* infection. (a) shows the sticky conidia and (b) shows the distribution of conidia and internal hyphae. IH internal hyphae, CS conidiospores, SPC sporangiophores with sticky conidia, SCW secondary cell wall, C conidia.

The SEM images of the analyzed *F. sycomorus* wood sample that was 5 mm deep and infected with *A. flavus* are displayed in Fig. 2a and b. The infected wood had *A. flavus* at its ideal density, which resulted in a notable increase in hyphal development and spore generation. After 36 months of incubation, *A. flavus* was detected inside the wood by CT scanning, as shown in Fig. 3.

The production of *A. flavus* conidial, however, may rise even below the surface, showing that *A. flavus* can rot *F. sycomorus* wood through the pits and within cell walls. Additionally, among the wood fibers, the spore and hyphae structure was visible. In a previous study, it was discovered that various molds, including *Botryodiplodia theobromae*, *Trichoderma longibrachiatum*, *A. candidus*, *A. ustus*, and *A. terreus* quickly degraded *F. sycomorus* wood³⁹. In addition to the great porosity of the wood, which allowed these aerobic fungi to grow through it, the low level of antimicrobial chemicals in *F. sycomorus* may have contributed to the enormous development of *A. flavus*³⁹.

Figure 4 depicts the SEM morphology of *P. chrysogenum* colonies on wood after 36 months at 27 ± 2 °C. It was possible to see *P. chrysogenum*, which had peridial hyphae with thick-walled dichotomously branching walls and a short, bifurcating appendage resembling a spine. The center displays a gymnothecium of the globose open reticulum type with ascospore mass. Ascospores and developing asci are seen. It is common to find tiny, radially projecting peridial appendages that resemble deer antlers.

In the wood of *F. sycomorus*, *P. chrysogenum* produced hair baits (Fig. 4a). The ascomata appeared to have septate, branching, and thick-walled peridial hyphae, but lacked the distinctive boathook-shaped appendages. Globose- to subglobose asci were present. Under SEM, the spores were seen to be irregular and rough (Fig. 4b through d).

In addition to severely degraded and weakened cell walls, SEM images of *F. sycomorus* wood degradation after 36 months also revealed colonized hyphae in cell walls. The total disintegration of the cell wall and vessels may be linked to the severe chemical materials degradation of the cell wall^{40–43}. As previously indicated, After 3 months of incubation with *A. niger*, identifiable notches of cell wall erosion and cavities created by fungal hyphae within the cell walls were discovered in wood, while *P. chrysogenum* only created erosion troughs formed in cell walls while colonizing *F. sycomorus* wood⁵.

SEM images of a 5-mm-deep incision in the infected wood were taken to demonstrate the extent of *P. chrysogenum* inside *F. sycomorus* wood (Fig. 5a through d). Images revealed *P. chrysogenum* inside wood had grown enormously. After 36 months of incubation, a CT scanning (Fig. 6) of the wood demonstrated *A. flavus* penetration growth.

The SEM images of wood samples from *F. sycomorus* showed that the cell walls were distorted, had some structures holes, and were missing entire wood cells. These are the results of the development of fungus hyphae and spores²⁹. Cell wall layers have likely detached and separated as a result of soft rot fungal growth^{20,44}. Despite poor structural preservation, a fungal microbial degradation was discovered in archeological *F. sycomorus* wood². After 4 months of incubation with *Penicillium chrysogenum*, the secondary wall layers of *F. sycomorus* wood were disrupted as a result of severe cell wall breakdown⁵.

SEM and CT scanning examination of incubated *Tectona grandis* wood. In all teak wood samples, the growth of *A. flavus* was minimized (Fig. 7a and b). The spore loss is visible in the SEM images. The branching and decay are the two main modifications to the hyphal morphology. According to Fig. 7c and d, phenolic and

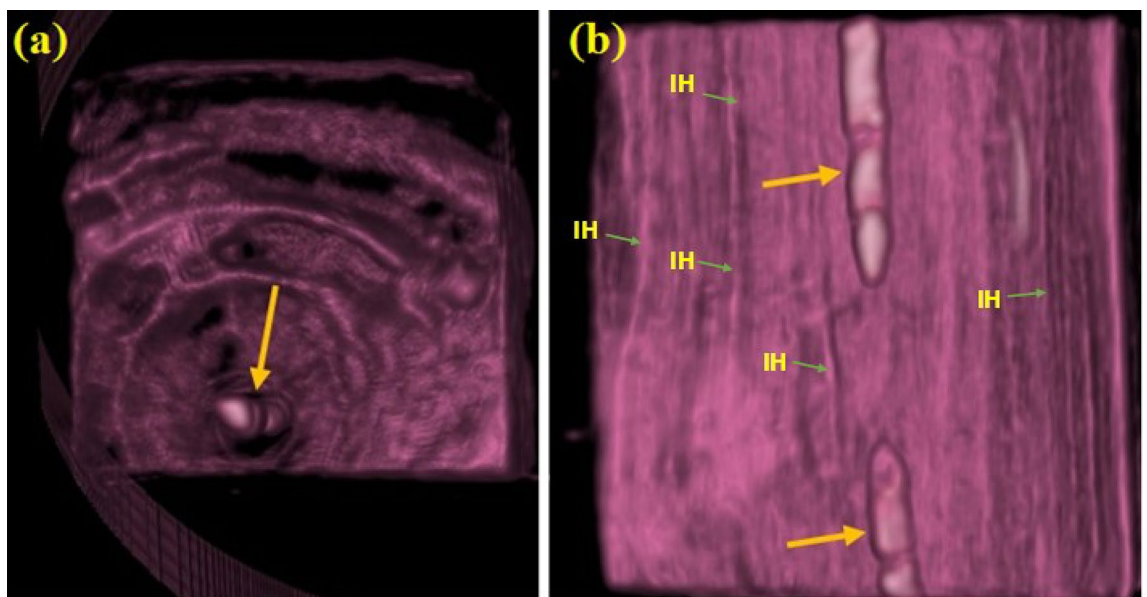


Figure 3. CT scan at cross-section (a) and longitudinal direction (b) of the inoculated *F. sycomorus* wood with *A. flavus* after 36 months; big arrows refer to insect-made pores; IH internal hyphae.

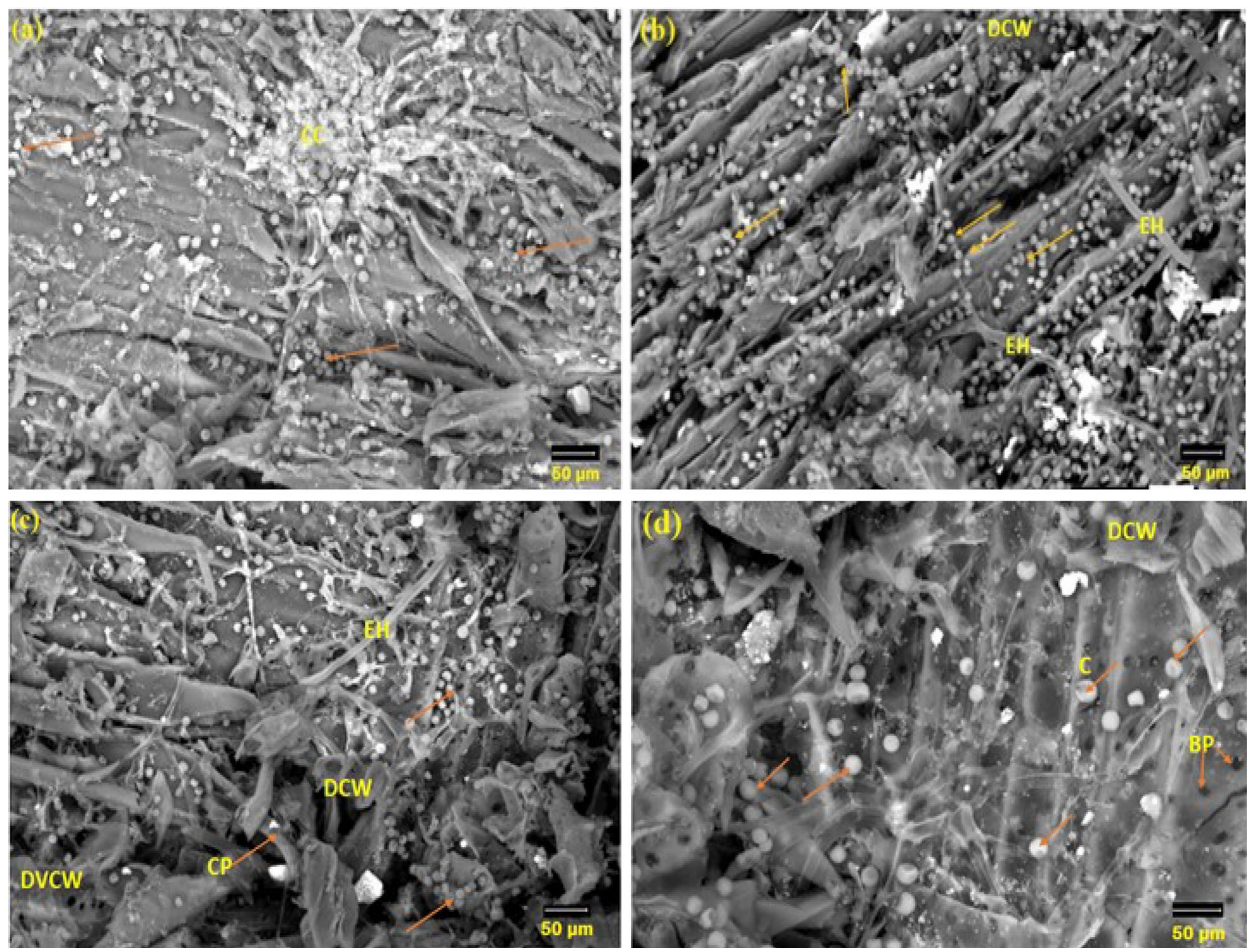


Figure 4. SEM surface features of *F. sycomorus* wood as inoculated with *P. chrysogenum* for 36 months, (a) shows the cluster of conidia, (b) shows the external hyphae with conidia, (c) shows the degraded vessel cell wall, and (d) shows the degraded cell wall. Arrows and circles refer to the intensive growth of *P. chrysogenum* (CC cluster of conidia, DCW degraded cell wall, EH external hyphae, C conidia, CP conidiophores, DVCW degraded vessel cell wall).

other aromatic antimicrobial chemicals prevent the growth of *A. flavus* on teak wood. Even after 36 months of incubation, the CT scanning (Fig. 8) supported the resistance patterns of teak wood to the spread of *A. flavus*.

After 36 months on incubation, teak wood infected with *Penicillium chrysogenum* showed reduced mycelial growth (Fig. 9a through d). These findings suggested that the conidial production of *P. chrysogenum* might not grow in teak wood due the presence of phenolic and other aromatic antimicrobial compounds, such as anthraquinones and tectoquinones^{45–50}. The chemical compounds in the wood changed the morphology of *P. chrysogenum*, colony morphology, and multicellular clumps that lost the spore.

It was discovered that the size of the mycelial pellets had significantly decreased, the cell wall had absorbed, and the shape of the mycelial pellets had changed. Nearly no growth indicators of *P. chrysogenum* were visible on the surface and core of the wood during the CT scanning (Fig. 10).

EDX measurements

Elemental composition changes of *Ficus sycomorus* wood. Incubated *F. sycomorus* wood with *A. flavus* and *P. chrysogenum* for 36 months is shown in Fig. 11 to have different elemental compositions from un-inoculated wood. In the un-inoculated wood (Fig. 11a and Table 1), The atomic percentages of C and O in the un-inoculated wood were 61.69%, and 37.81%, respectively, while they changed to 59.33% for C and 39.59% for O in the inoculated wood samples with *A. flavus* (Fig. 11b and Table 2). The C and O atomic percentages in wood samples inoculated with *P. chrysogenum* for 36 months dropped to 58.43%, and 26.34%, respectively (Fig. 11c and Table 3).

The un-inoculated wood contained 0.10% atomic percentage of K. In the infected wood with *A. flavus*, and *P. chrysogenum*, this climbed to 0.34% and 2.09%, respectively. Additionally, the Ca content rose from 0.18% in the control wood sample to 0.35% with *A. flavus* infected wood sample and to 1.81% in wood sample inoculated with *P. chrysogenum*.

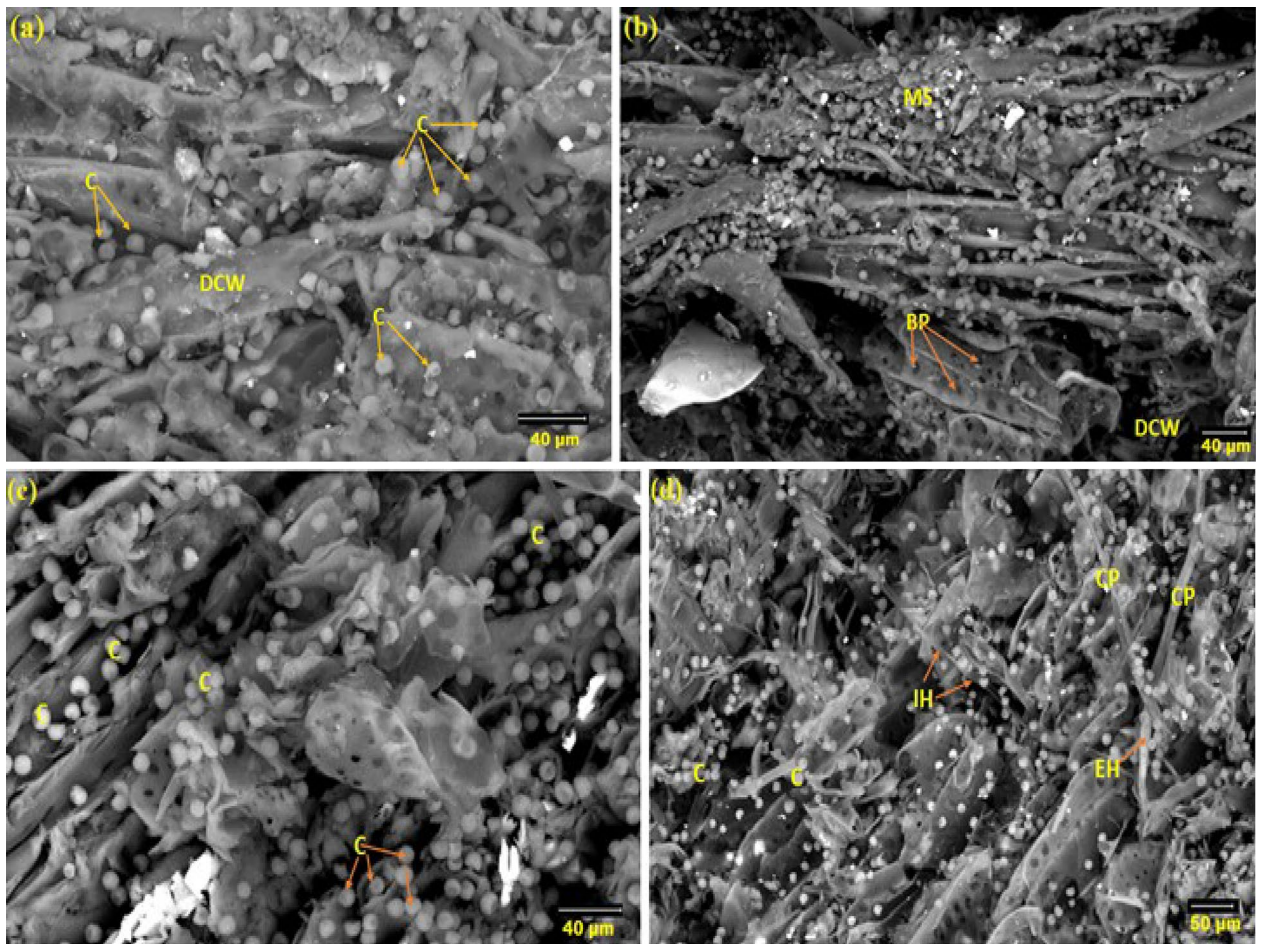


Figure 5. SEM micrograph of *F. sycomoros* after cutting 5-mm from infected wood and showing enlargement and deterioration of pits and detachment within cells due to *P. chrysogenum* attack and the spores and hyphae growth morphology are observed within the wood fibers: (a) shows the distribution of conidia and the degraded cell wall, (b) shows of mass of conidia, (c) shows the distribution of conidia, and (d) shows the Internal hyphae of *P. chrysogenum*. MS mass of conidia, DCW degraded cell wall, EH external hyphae, IH internal hyphae, C conidia, CP conidiophores.

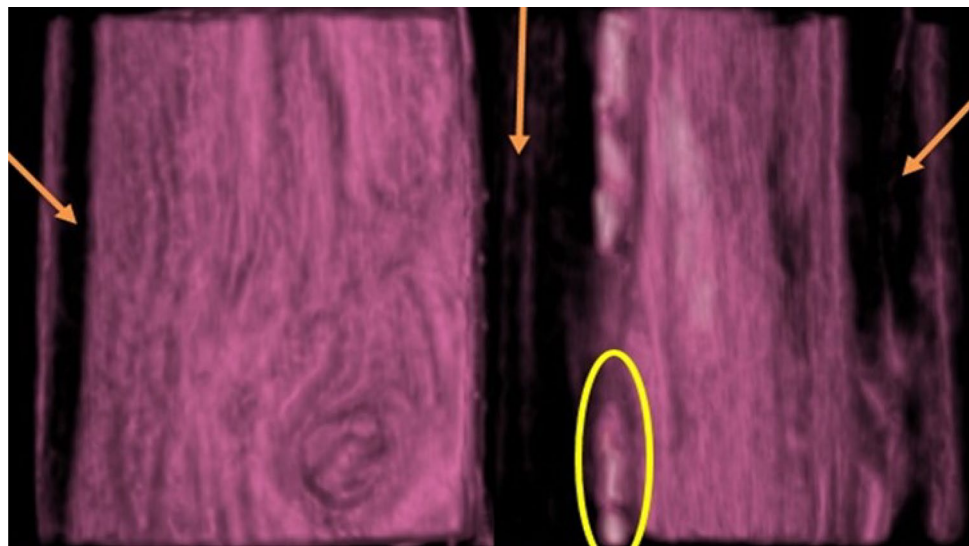


Figure 6. CT-scanning of *F. sycomoros* wood inoculated with *P. chrysogenum* for 36 months; arrows refer to the deterioration found in the wood after this long-term infection. The three arrows and circle depict the shapes of the longitudinal holes.

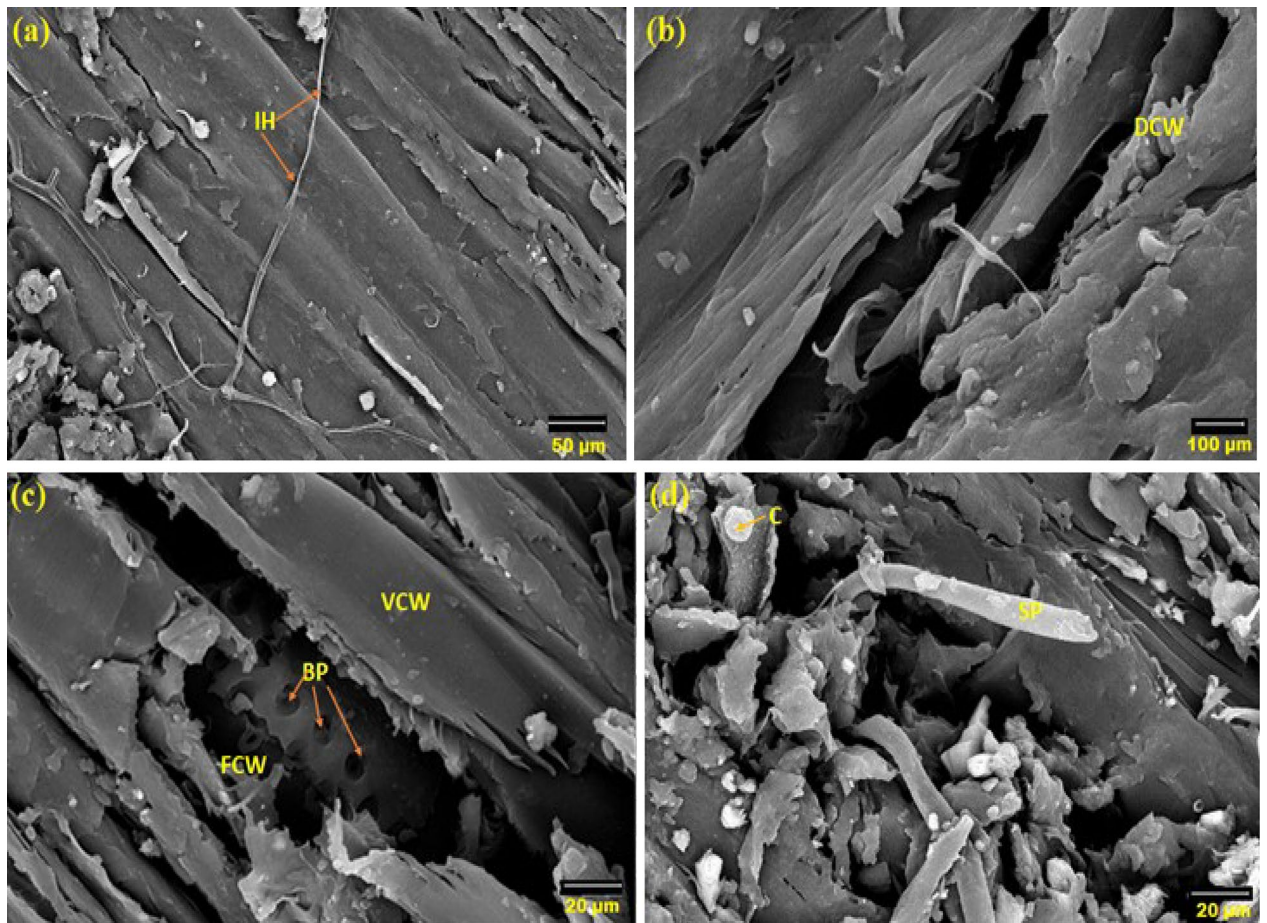


Figure 7. SEM images of teak wood that was surface-exposed to *A. flavus* for 36 months (a,b) and after cutting of 5-mm from infected wood (c,d). *IH* internal hyphae, *SP* sporangiophore, *C* conidium; *FCW* fiber cell wall, *VCW* vessel cell wall, *BP* bordered pits.

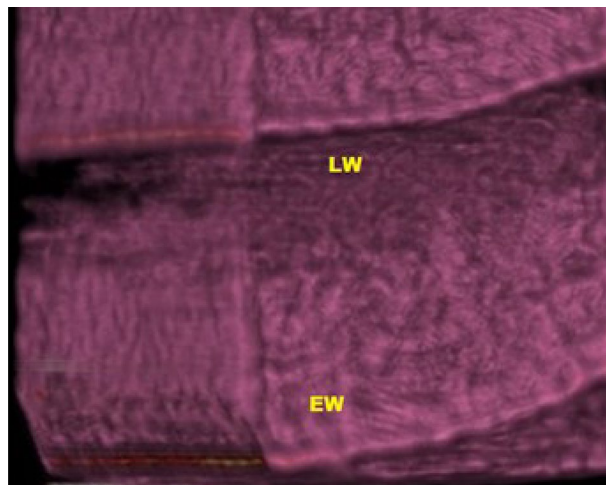


Figure 8. CT imaging of teak wood exposed to *A. flavus* after 36 months of incubation; *LW* latewood, *EW* early wood.

Elemental composition changes of teak wood. As compared to the un-inoculated sample, Fig. 12 illustrates the changes in the elemental composition of teak wood that was incubated for 36 months with *A. flavus* and *P. chrysogenum*. In the un-inoculated wood sample, C and O are the two most prevalent elements with atomic percentages of 70.85% and 28.78%, respectively (Fig. 12a and Table 4). As teak wood was inoculated with *A. flavus* (Fig. 12b and Table 5) and *P. chrysogenum* (Fig. 12c and Table 6) for 36 months, the atomic percent-

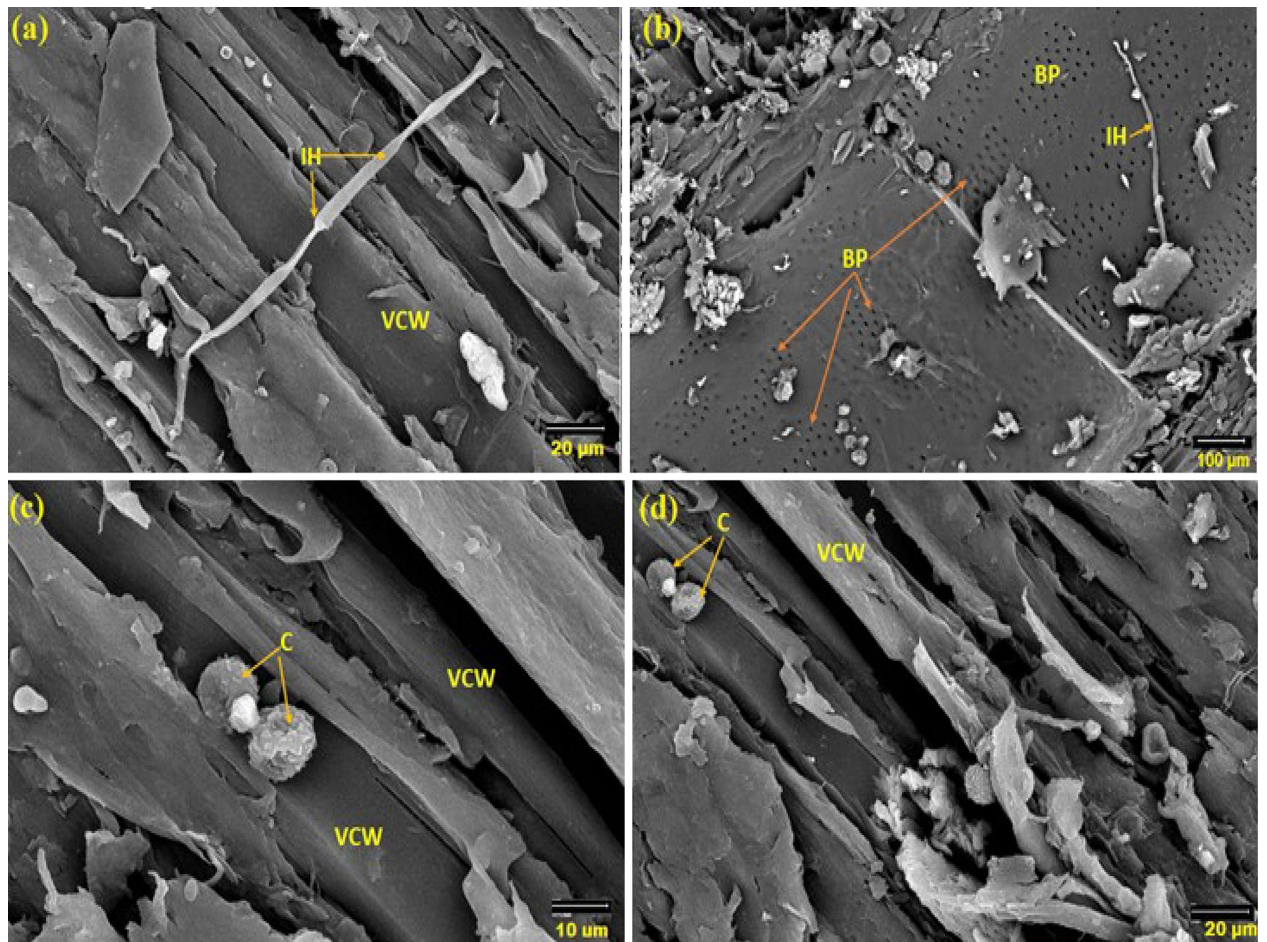


Figure 9. SEM micrograph of teak wood exposed to *P. chrysogenum* for 36 months on the surface (a,b) and at 0.5-mm depth of wood (c,d). *IH* internal hyphae, *C* conidium, *VCW* vessel cell wall, *BP* bordered pit.

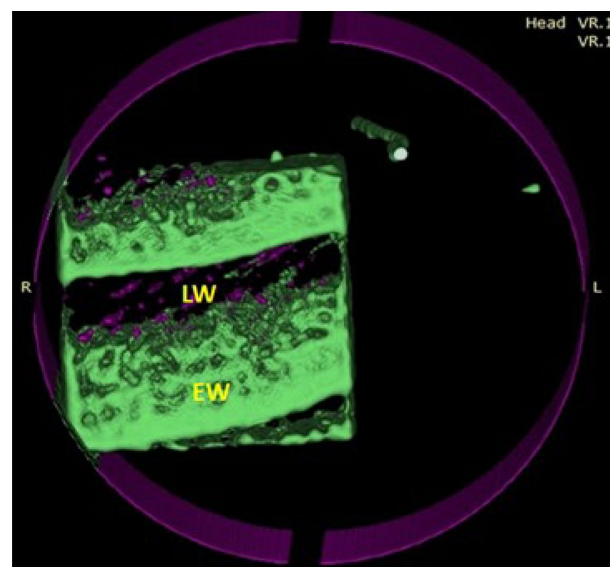


Figure 10. CT scanning of teak wood infected by *P. chrysogenum* after 36 months of the artificial inoculation. *LW* latewood, *EW* early wood.

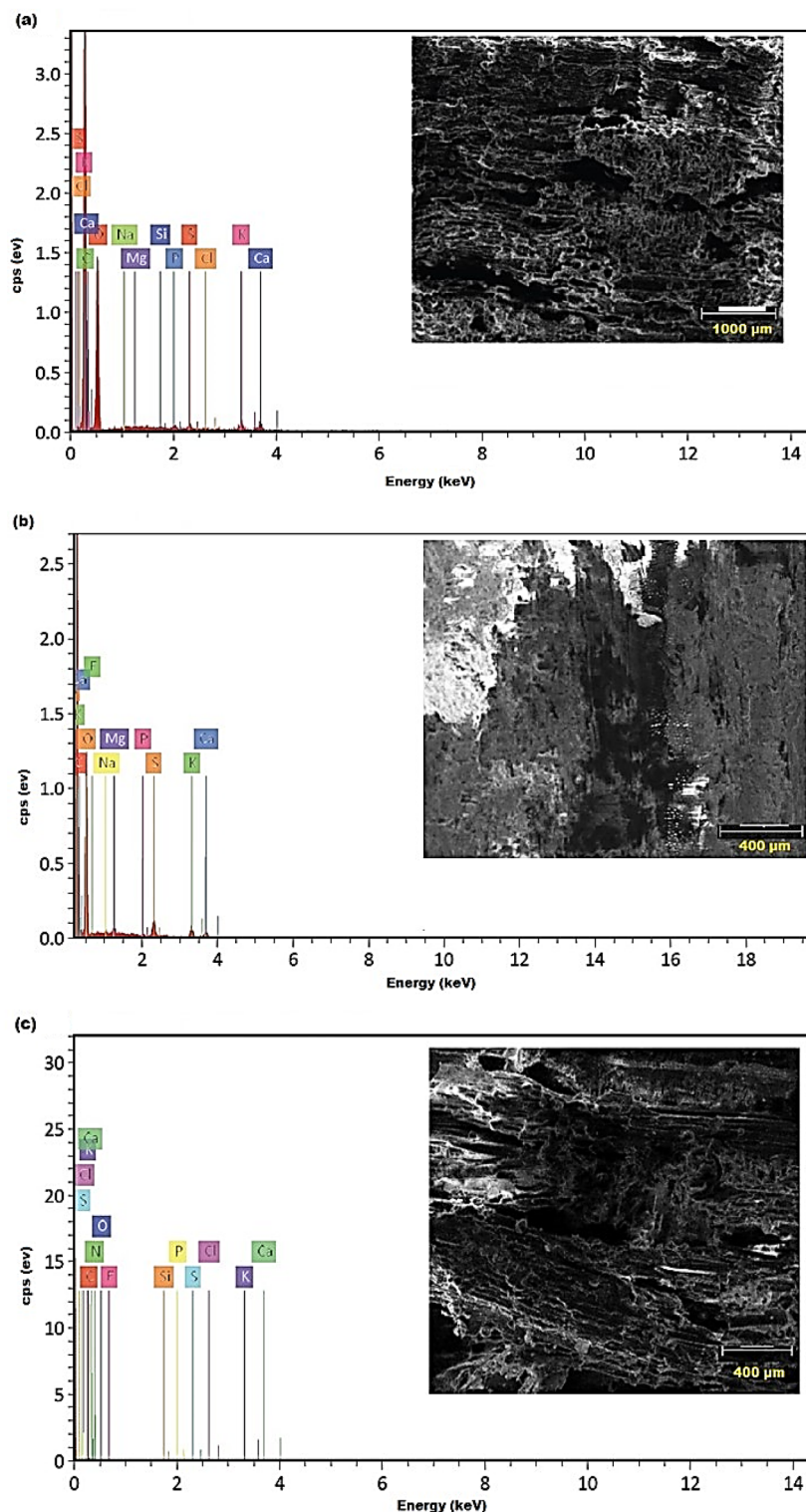


Figure 11. EDX spectral analysis of the elemental composition of un-inoculated *F. sycomorus* wood (a) and inoculated with *A. flavus* (b) and *P. chrysogenum* (c).

age of the C element decreased to 54.16% and 40.89%, respectively, while the O atomic percentage increased to 45.19% and 52.43%, respectively.

The authors found that there were both declines and increases in the concentration of various key components from the analytical results of the elemental compositions of the inoculated wood with the two molds under

Element	At. no	Netto	Mass (%)	Mass norm. (%)	Atom (%)
Carbon	6	15,310	54.33	54.33	61.69
Oxygen	8	7183	44.36	44.36	37.81
Calcium	20	583	0.53	0.53	0.18
Potassium	19	421	0.29	0.29	0.10
Sulfur	16	240	0.20	0.20	0.08
Phosphorus	15	170	0.13	0.13	0.06
Silicon	14	83	0.05	0.05	0.02
Chlorine	17	56	0.04	0.04	0.02
Magnesium	12	43	0.04	0.04	0.02
Sodium	11	29	0.04	0.04	0.02

Table 1. EDX elemental compositions of un-inoculated *Ficus sycomorus* wood.

Element	At. no	Netto	Mass (%)	Mass norm. (%)	Atom (%)
Carbon	6	11,702	51.46	51.46	59.33
Oxygen	8	5765	45.75	45.75	39.59
Calcium	20	342	1.02	1.02	0.35
Potassium	19	504	0.95	0.95	0.34
Sulfur	16	763	0.54	0.54	0.23
Magnesium	12	228	0.12	0.12	0.07
Sodium	11	120	0.08	0.08	0.05
Phosphorus	15	88	0.06	0.06	0.02
Fluorine	9	2	0.02	0.02	0.01

Table 2. EDX elemental compositions of *Ficus sycomorus* wood inoculated with *Aspergillus flavus*.

Element	At. no	Netto	Mass (%)	Mass norm. (%)	Atom (%)
Carbon	6	651	5.88	47.97	58.43
Oxygen	8	134	3.53	28.81	26.34
Nitrogen	7	15	1.04	8.52	8.90
Potassium	19	252	0.69	5.60	2.09
Calcium	20	221	0.61	4.96	1.81
Fluorine	9	10	0.21	1.72	1.32
Sulfur	16	24	0.11	0.90	0.41
Chlorine	17	20	0.09	0.73	0.30
Phosphorus	15	12	0.06	0.50	0.23
Silicon	14	8	0.04	0.31	0.16

Table 3. EDX elemental compositions of *Ficus sycomorus* wood inoculated with *Penicillium chrysogenum*.

study. Molds are typically discovered and grow in moisture-damaged wood⁵¹, create colored spores and large amounts of pigment on the surfaces of wood, which decrease the quality of the wood^{52,53}, but do not influence the strength of the wood⁵⁴.

The carbon-rich components of wood are reported to be metabolized by molds and fungi that disintegrate wood. This produces massive fruiting structures of fungi, which release a huge amount of spores into the natural environment^{10,55}. Molds that are unable to depolymerize the primary chemical polymers of wood (cellulose, lignin and hemicelluloses) can consume the sugars and starches found in ray and axial parenchyma cells lumen⁵⁶. Through pores and pits, The hyphae of the fungus can enter the cell walls through holes and crevices⁵⁷.

The two mold fungi-inoculated woods showed that the C element content was lower than it was in the control sample. This outcome is consistent with previous work¹⁰. Additionally, it was found that the molds absorbed the C sources⁵⁸. When growing on *Fagus sylvatica* wood, molds like *P. selerotigenum* and *A. niger* consume a lot of C, but *P. selerotigenum* consumes a lot of C content when growing on *Juglans nigra* wood. In contrast, minimal

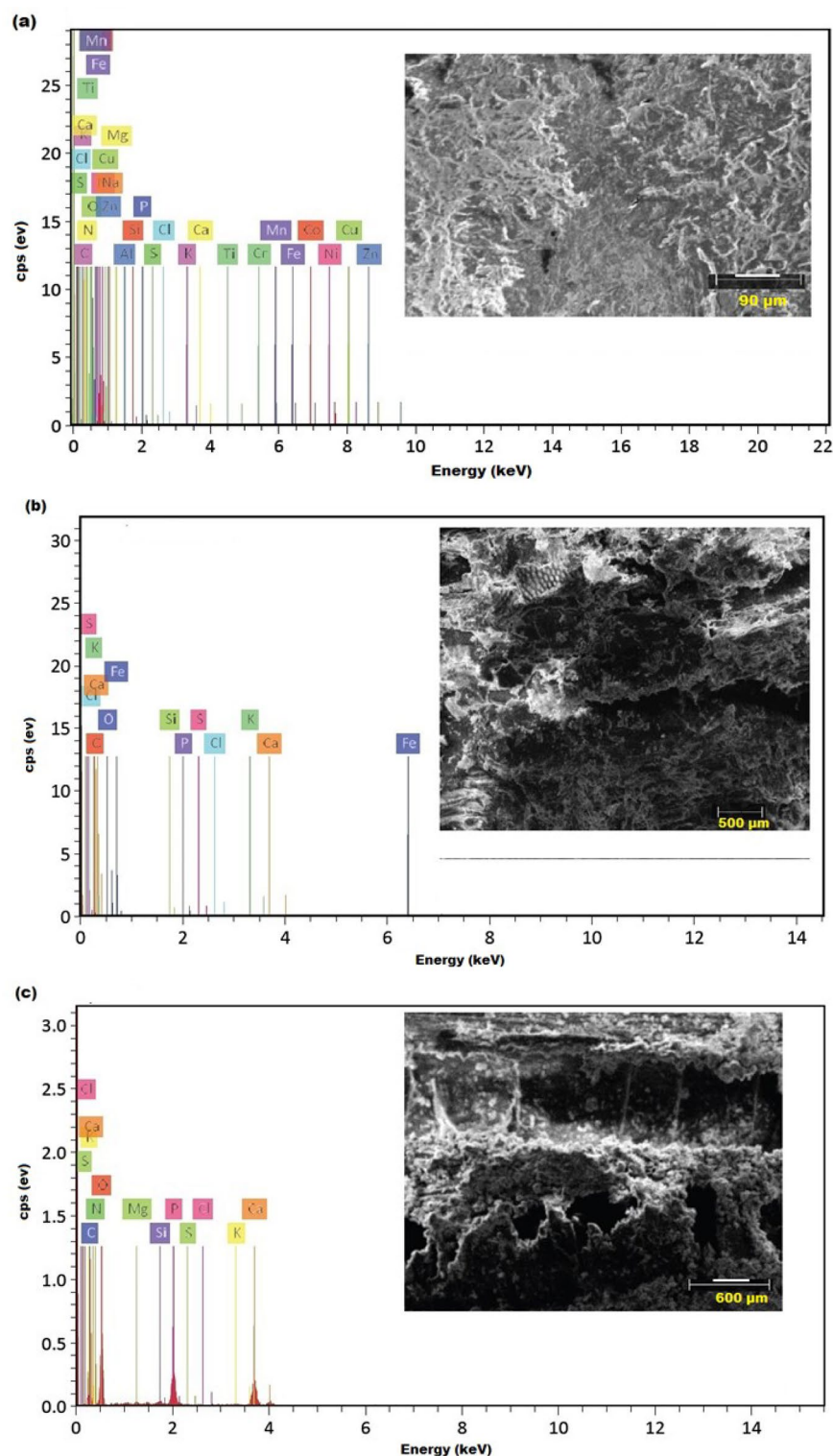


Figure 12. The elemental composition of un-inoculated teak wood analyzed using EDX spectroscopy. (a), inoculated with *A. flavus* (b) and inoculated with *P. chrysogenum* (c).

change in C content of *P. rigida* wood was observed when colonized by *P. sclerotigenum*, *Paecilomyces variotii*, and *A. niger*, on the other hand, caused no change in the C content of *P. rigida* wood⁷.

According to the tests of adhesion in the study of Soumya et al.⁵⁹, *P. chrysogenum* was unable to adhere to the cedar wood substrate, although *P. granulatum*, *P. crustosum*, and *P. commune* were able to do so, contrary to what was theoretically expected. The development of *P. chrysogenum* PCL501 on wood waste results in the production of the xylanase enzyme, which is most strongly induced by the carbon source⁶⁰. When cultured on a

Element	At. no	Netto	Mass (%)	Mass norm. (%)	Atom (%)
Carbon	6	12,351	64.21	64.21	70.85
Oxygen	8	3044	34.74	34.74	28.78
Calcium	20	267	0.41	0.41	0.14
Iron	26	46	0.24	0.24	0.06
Potassium	19	67	0.07	0.07	0.02
Sodium	11	43	0.05	0.05	0.03
Fluorine	9	5	0.05	0.05	0.03
Sulfur	16	52	0.04	0.04	0.02
Magnesium	12	43	0.04	0.04	0.02
Cobalt	27	4	0.03	0.03	0.01
Silicon	14	47	0.03	0.03	0.01
Chlorine	17	30	0.02	0.02	0.01
Manganese	25	5	0.02	0.02	0.01
Nickel	28	2	0.02	0.02	0.00
Aluminium	13	21	0.02	0.02	0.01
Phosphorus	15	17	0.01	0.01	0.00
Nitrogen	7	0	0.00	0.00	0.00
Titanium	22	0	0.00	0.00	0.00

Table 4. EDX elemental compositions of un-inoculated teak wood.

Element	At. no	Netto	Mass (%)	Mass norm. (%)	Atom (%)
Oxygen	8	7196	51.57	51.73	45.19
Carbon	6	10,318	46.40	46.54	54.16
Calcium	20	413	0.82	0.82	0.29
Silicon	14	415	0.33	0.33	0.16
Potassium	19	166	0.28	0.28	0.10
Chlorine	17	104	0.12	0.13	0.05
Iron	26	19	0.10	0.10	0.02
Sulfur	16	63	0.06	0.06	0.03
Phosphorus	15	6	0.01	0.01	0.00

Table 5. EDX elemental compositions of teak wood inoculated with *Aspergillus flavus*.

Element	At. no	Netto	Mass (%)	Mass norm. (%)	Atom (%)
Oxygen	8	3179	47.98	53.83	52.43
Carbon	6	1936	28.09	31.51	40.89
Calcium	20	1978	7.11	7.97	3.10
Phosphorus	15	2081	4.96	5.56	2.80
Magnesium	12	106	0.33	0.37	0.24
Nitrogen	7	6	0.25	0.28	0.31
Silicon	14	114	0.22	0.25	0.14
Potassium	19	41	0.12	0.13	0.05
Sulfur	16	19	0.05	0.06	0.03
Chlorine	17	10	0.03	0.04	0.02

Table 6. EDX elemental compositions of teak wood inoculated with *Penicillium chrysogenum*.

bran-wood flour-olive oil or a bran-soy bean media, the water-soluble enzyme (Lipase) generated by *P. oxalicum* and *A. flavus* was capable of hydrolyzing the olive oil⁶¹.

The lignin structure in agricultural lignocellulosic wastes was discovered to be degraded by the strain of *A. flavus* EGYPTA5, which secretes lignin peroxidases, nitrate reductase, laccase, polyphenol oxidase, and cellulase enzymes, without changing the concentration of cellulose⁶². It was discovered that several *A. flavus* fungal

isolates produced cellulase-free xylanase in a variety of soil environments, including manures, dead and decaying wood, and soil samples⁶³. *A. flavus* produced the most cellulase enzyme when it was cultivated on wood sawdust, according to study⁶⁴. *A. flavus* was isolated from its natural environment including wastewater, rotting wood, wheat straw, and field soil samples, and it produced laccase enzyme⁶⁵.

Both SEM and CT scanning examinations confirmed the growth of molds on the studied wood samples on the surface and core showing the structural growth of fungi.

Conclusions

The dispersion of the two molds' fruiting structures, spores, and hyphae that covered the damaged wood surfaces after 36 months of incubation could be clearly seen by the examination instruments SEM-EDX and CT scanning. According to the study, the carbon-rich components of the examined *Ficus sycomorus* and *Tectona grandis* woods are metabolized proportionately by *Aspergillus flavus* and *Penicillium chrysogenum*. The findings supported the long-term durability and the non-durability phenomena of *Tectona grandis* and *Ficus sycomorus* woods, respectively. Finally, the surface and core of the analyzed wood samples showed structural growth of fungi, which was validated by SEM and CT scanning studies.

Data availability

All data generated or analyzed during this study are included in this published article.

Received: 11 March 2023; Accepted: 22 June 2023

Published online: 28 June 2023

References

1. Abdallah, M. & Abdrabou, A. Tutankhamen's small shrines (naoses): Technology of woodworking and identification of wood species. *Int. J. Conserv. Sci.* **9**, 91–104 (2018).
2. Tamburini, D. *et al.* A critical evaluation of the degradation state of dry archaeological wood from Egypt by SEM, ATR-FTIR, wet chemical analysis and Py(HMDS)-GC-MS. *Polym. Degrad. Stab.* **146**, 140–154. <https://doi.org/10.1016/j.polymdegradstab.2017.10.009> (2017).
3. Blanchette, R. A., Obst, J. R., Hedges, J. I. & Weliky, K. Resistance of hardwood vessels to degradation by white rot Basidiomycetes. *Can. J. Bot.* **66**, 1841–1847. <https://doi.org/10.1139/b88-251> (1988).
4. Yang, B., Dai, Z., Ding, S.-Y. & Wyman, C. E. Enzymatic hydrolysis of cellulosic biomass. *Biofuels* **2**, 421–449. <https://doi.org/10.4155/bfs.11.116> (2011).
5. Hamed, S. A. M. In-vitro studies on wood degradation in soil by soft-rot fungi: *Aspergillus niger* and *Penicillium chrysogenum*. *Int. Biodeter. Biodegrad.* **78**, 98–102. <https://doi.org/10.1016/j.ibiod.2012.12.013> (2013).
6. Hosseinihashemi, S. K., Salem, M. Z. M., HosseinAshrafi, S. K. & Jahan Latibari, A. Chemical composition and antioxidant activity of extract from the wood of *Fagus orientalis*: Water resistance and decay resistance against *Trametes versicolor*. *BioResources* **11**, 3890–3903. <https://doi.org/10.15376/biores.11.2.3890-3903> (2016).
7. Salem, M. Z. M. EDX measurements and SEM examination of surface of some imported woods inoculated by three mold fungi. *Measurement* **86**, 301–309. <https://doi.org/10.1016/j.measurement.2016.03.008> (2016).
8. Hamed, S. & Mansour, M. M. A. Comparative study on micromorphological changes in wood due to soft-rot fungi and surface mold. *Sci. Cult.* **4**, 35–41. <https://doi.org/10.5281/zenodo.1214563> (2018).
9. Mansour, M. M., El-Hefny, M., Salem, M. Z. & Ali, H. M. The biofungicide activity of some plant essential oils for the cleaner production of model linen fibers similar to those used in ancient Egyptian mummification. *Processes* **8**, 79. <https://doi.org/10.3390/pr8010079> (2020).
10. Mansour, M. M. A. & Salem, M. Z. M. Evaluation of wood treated with some natural extracts and Paraloid B-72 against the fungus *Trichoderma harzianum*: Wood elemental composition, in-vitro and application evidence. *Int. Biodeter. Biodegrad.* **100**, 62–69. <https://doi.org/10.1016/j.ibiod.2015.02.009> (2015).
11. Blaich, R. & Esser, K. Function of enzymes in wood destroying fungi. *Arch. Microbiol.* **103**, 271–277. <https://doi.org/10.1007/BF00436360> (1975).
12. Dean, R. A. & Timberlake, W. E. Production of cell wall-degrading enzymes by *Aspergillus nidulans*: A model system for fungal pathogenesis of plants. *Plant Cell* **1**, 265–273. <https://doi.org/10.1105/tpc.1.3.265> (1989).
13. Wood, T. M. & McCrae, S. I. Arabinoxylan-degrading enzyme system of the fungus *Aspergillus awamori*: Purification and properties of an α -l-arabinofuranosidase. *Appl. Microbiol. Biotechnol.* **45**, 538–545. <https://doi.org/10.1007/BF00578468> (1996).
14. Gramss, G., Ziegenhagen, D. & Sorge, S. Degradation of soil humic extract by wood- and soil-associated fungi, bacteria, and commercial enzymes. *Microb. Ecol.* **37**, 140–151. <https://doi.org/10.1007/s002489900138> (1999).
15. Hu, H. L. *et al.* Improved enzyme production by co-cultivation of *Aspergillus niger* and *Aspergillus oryzae* and with other fungi. *Int. Biodeter. Biodegrad.* **65**, 248–252. <https://doi.org/10.1016/j.ibiod.2010.11.008> (2011).
16. Monroy, M., Ortega, I., Ramírez, M., Baeza, J. & Freer, J. Structural change in wood by brown rot fungi and effect on enzymatic hydrolysis. *Enzyme Microb. Technol.* **49**, 472–477. <https://doi.org/10.1016/j.enzmictec.2011.08.004> (2011).
17. Yang, D.-Q. Staining ability of various sapstaining fungi on Jack pine short log sections. *For. Prod. J.* **51**, 73–73 (2001).
18. Fuhr, M. J., Schubert, M., Schwarze, F. W. M. R. & Herrmann, H. J. Modelling the hyphal growth of the wood-decay fungus *Physisporinus vitreus*. *Fungal Biol.* **115**, 919–932. <https://doi.org/10.1016/j.funbio.2011.06.017> (2011).
19. Salem, M. Z. M., Mansour, M. M. A. & Elansary, H. O. Evaluation of the effect of inner and outer bark extracts of sugar maple (*Acer saccharum* var. *saccharum*) in combination with citric acid against the growth of three common molds. *J. Wood Chem. Technol.* **39**, 136–147. <https://doi.org/10.1080/02773813.2018.1547763> (2019).
20. Schwarze, F. W. M. R. Wood decay under the microscope. *Fungal Biol. Rev.* **21**, 133–170. <https://doi.org/10.1016/j.fbr.2007.09.001> (2007).
21. Daniel, G. *Secondary Xylem Biology* 131–167 (Academic Press, 2016).
22. Morris, H., Brodersen, C., Schwarze, F. W. M. R. & Jansen, S. The parenchyma of secondary xylem and its critical role in tree defense against fungal decay in relation to the CODIT model. *Front. Plant Sci.* **7**, 1665. <https://doi.org/10.3389/fpls.2016.01665> (2016).
23. Krogh, K. B. R., Mørkeberg, A., Jørgensen, H., Frisvad, J. C. & Olsson, L. In *Proceedings of the Twenty-Fifth Symposium on Biotechnology for Fuels and Chemicals Held May 4–7, 2003, in Breckenridge, CO* (eds Mark Finkelstein, James D. McMillan, Brian H. Davison, & Barbara Evans) 389–401 (Humana Press).
24. Yoon, J. H., Hong, S. B., Ko, S. J. & Kim, S. H. Detection of extracellular enzyme activity in *Penicillium* using chromogenic media. *Mycobiology* **35**, 166–169. <https://doi.org/10.4489/MYCO.2007.35.3.166> (2007).

25. de Vries Ronald, P. & Visser, J. *Aspergillus* enzymes involved in degradation of plant cell wall polysaccharides. *Microbiol. Mol. Biol. Rev.* **65**, 497–522. <https://doi.org/10.1128/MMBR.65.4.497-522.2001> (2001).
26. Horn, S. J., Vaaje-Kolstad, G., Westereng, B. & Eijsink, V. Novel enzymes for the degradation of cellulose. *Biotechnol. Biofuels* **5**, 45. <https://doi.org/10.1186/1754-6834-5-45> (2012).
27. Unger, A., Schniewind, A. & Unger, W. *Conservation of Wood Artifacts: A Handbook* 578 (Springer Science & Business Media, Science, 2001).
28. Mansour, M. M., Hamed, S.A.E.-K.M., Salem, M. Z. & Ali, H. M. Illustration of the effects of five fungi on *Acacia saligna* wood organic acids and ultrastructure alterations in wood cell walls by HPLC and TEM examinations. *Appl. Sci.* **10**, 2886. <https://doi.org/10.3390/app10082886> (2020).
29. Popescu, C.-M., Dobeles, G., Rossinskaja, G., Dizhbite, T. & Vasile, C. Degradation of lime wood painting supports: Evaluation of changes in the structure of aged lime wood by different physico-chemical methods. *J. Anal. Appl. Pyrolysis* **79**, 71–77. <https://doi.org/10.1016/j.jaap.2006.12.014> (2007).
30. Bucur, V. *Nondestructive Characterization and Imaging of Wood* 354 (Springer Science & Business Media, Technology & Engineering, 2003).
31. Brodersen, C. R. *et al.* Automated analysis of three-dimensional xylem networks using high-resolution computed tomography. *New Phytol.* **191**, 1168–1179. <https://doi.org/10.1111/j.1469-8137.2011.03754.x> (2011).
32. Schimleck, L. *et al.* Non-destructive evaluation techniques and what they tell us about wood property variation. *Forests* **10**, 728. <https://doi.org/10.3390/f10090728> (2019).
33. Abo Elgat, W. A. *et al.* The effects of iron rust on the ageing of woods and their derived pulp paper. *Polymers* **13**, 3483. <https://doi.org/10.3390/polym13203483> (2021).
34. Salem, M. Z. M., Zidan, Y. E., El Hadidi, N. M. N., Mansour, M. M. A. & Abo Elgat, W. A. A. Evaluation of usage three natural extracts applied to three commercial wood species against five common molds. *Int. Biodeter. Biodegrad.* **110**, 206–226. <https://doi.org/10.1016/j.ibiod.2016.03.028> (2016).
35. Mohamed, W. A., Mansour, M. M. A. & Salem, M. Z. M. *Lemna gibba* and *Eichhornia crassipes* extracts: Clean alternatives for deacidification, antioxidation and fungicidal treatment of historical paper. *J. Clean. Prod.* **219**, 846–855. <https://doi.org/10.1016/j.jclepro.2019.02.097> (2019).
36. Mansour, M. Impact of storage conditions on biodeterioration of ancient Egyptian child mummies by Xerophilic Fungi. *Egypt. J. Archaeol. Restor. Stud.* **8**, 97–107 (2018).
37. Mohamed, W. A., Mansour, M. M. A., Salem, M. Z. M., Ali, H. M. & Böhm, M. X-ray computed tomography (CT) and ESEM-EDS investigations of unusual subfossilized juniper cones. *Sci. Rep.* **11**, 22308. <https://doi.org/10.1038/s41598-021-01789-z> (2021).
38. Kotwaliwale, N. *et al.* X-ray imaging methods for internal quality evaluation of agricultural produce. *J. Food Sci. Technol.* **51**, 1–15. <https://doi.org/10.1007/s13197-011-0485-y> (2014).
39. Darwish, S. S., EL Hadidi, N. & Mansour, M. M. A. The effect of fungal decay on *Ficus sycomorus* wood. *Int. J. Conserv. Sci.* **4**, 271–282 (2013).
40. Bari, E. *et al.* Decay of *Carpinus betulus* wood by *Trametes versicolor*—An anatomical and chemical study. *Int. Biodeter. Biodegrad.* **137**, 68–77. <https://doi.org/10.1016/j.ibiod.2018.11.011> (2019).
41. Bari, E. *et al.* Monitoring the cell wall characteristics of degraded beech wood by white-rot fungi: Anatomical, chemical, and photochemical study. *Maderas Cien. Tecnol.* **20**, 35–56. <https://doi.org/10.4067/S0718-221X2018005001401> (2018).
42. Bari, E. *et al.* Comparison between degradation capabilities of the white rot fungi *Pleurotus ostreatus* and *Trametes versicolor* in beech wood. *Int. Biodeter. Biodegrad.* **104**, 231–237. <https://doi.org/10.1016/j.ibiod.2015.03.033> (2015).
43. Kim, J. S., Gao, J. & Daniel, G. Cytochemical and immunocytochemical characterization of wood decayed by the white rot fungus *Pycnoporus sanguineus* II. Degradation of lignin and non-cellulosic polysaccharides in European ash wood. *Int. Biodeter. Biodegrad.* **105**, 41–50. <https://doi.org/10.1016/j.ibiod.2015.08.009> (2015).
44. Blanchette, R. A. A review of microbial deterioration found in archaeological wood from different environments. *Int. Biodeter. Biodegrad.* **46**, 189–204. [https://doi.org/10.1016/S0964-8305\(00\)00077-9](https://doi.org/10.1016/S0964-8305(00)00077-9) (2000).
45. Scheffer, T. C. Natural resistance of wood to microbial deterioration. *Annu. Rev. Phytopathol.* **4**, 147–168. <https://doi.org/10.1146/annurev.py.04.090166.001051> (1966).
46. Kokutse, A. D., Stokes, A., Baillères, H., Kokou, K. & Baudasse, C. Decay resistance of Togolese teak (*Tectona grandis* L.f) heartwood and relationship with colour. *Trees* **20**, 219–223. <https://doi.org/10.1007/s00468-005-0028-0> (2006).
47. Thulasidas, P. K. & Bhat, K. M. Chemical extractive compounds determining the brown-rot decay resistance of teak wood. *Holz a Roh- u. Werkst.* **65**, 121–124. <https://doi.org/10.1007/s00107-006-0127-7> (2007).
48. Brocco, V. F., Paes, J. B., Costa, L. G. D., Brazolin, S. & Arantes, M. D. C. Potential of teak heartwood extracts as a natural wood preservative. *J. Clean. Prod.* **142**, 2093–2099. <https://doi.org/10.1016/j.jclepro.2016.11.074> (2017).
49. Rodríguez Anda, R. *et al.* Formation of heartwood, chemical composition of extractives and natural durability of plantation-grown teak wood from Mexico. *Holzforschung* **73**, 547–557. <https://doi.org/10.1515/hf-2018-0109> (2019).
50. Broda, M. Natural compounds for wood protection against fungi—A review. *Molecules* **25**, 3538. <https://doi.org/10.3390/molecules25153538> (2020).
51. Hukka, A. & Viitanen, H. A. A mathematical model of mould growth on wooden material. *Wood Sci. Technol.* **33**, 475–485. <https://doi.org/10.1007/s002260050131> (1999).
52. Viitanen, H. & Ritschkoff, A.-C. *Mould Growth in Pine and Spruce Sapwood in Relation to Air Humidity and Temperature* (Swedish University of Agricultural Sciences, 1991).
53. Ghosh, S. C., Militz, H. & Mai, C. The efficacy of commercial silicones against blue stain and mould fungi in wood. *Eur. J. Wood Wood Prod.* **67**, 159–167. <https://doi.org/10.1007/s00107-008-0296-7> (2009).
54. Daniel, G. *Wood Deterioration and Preservation* Vol. 845, 34–72 (American Chemical Society, 2003).
55. Mansour, M. M., Abdel-Megeed, A., Nasser, R. A. & Salem, M. Z. M. Comparative evaluation of some woody tree methanolic extracts and Paraloid B-72 against phytopathogenic mold fungi *Alternaria tenuissima* and *Fusarium culmorum*. *BioResources* **10**, 2570–2584. <https://doi.org/10.15376/biores.10.2.2570-2584> (2015).
56. Kerner-Gang, W. & Schneider, R. V. Optischen Gläsern isolierte Schimmelpilze. *Mater. Organismen Mater. Organ. Matériaux Organismes* **4**, 291–296 (1969).
57. Eriksson, K.-E.L., Blanchette, R. A. & Ander, P. *Microbial and Enzymatic Degradation of Wood and Wood Components* (Springer Science & Business Media, 2012).
58. Komon-Zelazowska, M. *et al.* Genetically closely related but phenotypically divergent *Trichoderma* species cause green mold disease in oyster mushroom farms worldwide. *Appl. Environ. Microbiol.* **73**, 7415–7426. <https://doi.org/10.1128/aem.01059-07> (2007).
59. Soumya, E., Saad, I. K., Abdellah, H. & Hassan, L. Experimental and theoretical investigations of the adhesion time of *Penicillium* spores to cedar wood surface. *Mater. Sci. Eng. C* **33**, 1276–1281. <https://doi.org/10.1016/j.msec.2012.12.026> (2013).
60. Okafor, U., Emezue, T., Okochi, V., Onyegeme-Okerenta, B. & Nwodo-Chinedu, S. Xylanase production by *Penicillium chrysogenum* (PCL501) fermented on cellulosic wastes. *Afr. J. Biochem. Res.* **1**, 048–053 (2007).
61. Kirsh, D. Lipase production by *Penicillium oxalicum* and *Aspergillus flavus*. *Bot. Gaz.* **97**, 321–333. <https://doi.org/10.1086/334555> (1935).

62. Hasanin, M. S., Darwesh, O. M., Matter, I. A. & El-Saied, H. Isolation and characterization of non-cellulolytic *Aspergillus flavus* EGYPTA5 exhibiting selective ligninolytic potential. *Biocatal. Agric. Biotechnol.* **17**, 160–167. <https://doi.org/10.1016/j.bcab.2018.11.012> (2019).
63. Gautam, A., Kumar, A. & Dutt, D. Production of cellulase-free xylanase by *Aspergillus flavus* ARC-12 using pearl millet stover as the substrate under solid-state fermentation. *J. Adv. Enzym. Res.* **1**, 1–9 (2015).
64. Ojumu, T. V., Solomon, B. O., Betiku, E., Layokun, S. K. & Amigun, B. Cellulase production by *Aspergillus flavus* Linn isolate NSPR 101 fermented in sawdust, bagasse and corncob. *Afr. J. Biotechnol.* **2**, 150–152. <https://doi.org/10.5897/AJB2003.000-1030> (2003).
65. Kumar, R., Kaur, J., Jain, S. & Kumar, A. Optimization of laccase production from *Aspergillus flavus* by design of experiment technique: Partial purification and characterization. *J. Genet. Eng. Biotechnol.* **14**, 125–131. <https://doi.org/10.1016/j.jgeb.2016.05.006> (2016).

Author contributions

M.M.A.M., M.Z.M.S. and M.G.S.F. investigation, formal analysis, and resources. M.M.A.M., W.A.M., A.A.A.E.-S., M.B., M.Z.M.S. and M.G.S.F. contributed to conceptualization, methodology, writing, review, and editing. All authors read and approved the final manuscript.

Funding

Open access funding provided by The Science, Technology & Innovation Funding Authority (STDF) in cooperation with The Egyptian Knowledge Bank (EKB).

Competing interests

The authors declare no competing interests.

Additional information

Correspondence and requests for materials should be addressed to M.M.A.M. or M.Z.M.S.

Reprints and permissions information is available at www.nature.com/reprints.

Publisher's note Springer Nature remains neutral with regard to jurisdictional claims in published maps and institutional affiliations.



Open Access This article is licensed under a Creative Commons Attribution 4.0 International License, which permits use, sharing, adaptation, distribution and reproduction in any medium or format, as long as you give appropriate credit to the original author(s) and the source, provide a link to the Creative Commons licence, and indicate if changes were made. The images or other third party material in this article are included in the article's Creative Commons licence, unless indicated otherwise in a credit line to the material. If material is not included in the article's Creative Commons licence and your intended use is not permitted by statutory regulation or exceeds the permitted use, you will need to obtain permission directly from the copyright holder. To view a copy of this licence, visit <http://creativecommons.org/licenses/by/4.0/>.

© The Author(s) 2023